Histochem Cell Biol (2006) 125: 487–495
DOI 10.1007/s00418-005-0138-1

ORIGINAL PAPER

**Helene M. Langevin · Kirsten N. Storch
Marilyn J. Cipolla · Sheryl L. White
Thomas R. Buttolph · Douglas J. Taatjes**

Fibroblast spreading induced by connective tissue stretch involves intracellular redistribution of α- and β-actin

Accepted: 6 December 2005 / Published online: 14 January 2006

Abstract Mechanical stretching of connective tissue occurs with normal movement and postural changes, as well as treatments including physical therapy, massage and acupuncture. Connective tissue fibroblasts were recently shown to respond actively to short-term mechanical stretch (minutes to hours) with reversible cytoskeletal remodeling, characterized by extensive cell spreading and lamellipodia formation. In this study, we have examined the effect of tissue stretch on the distribution of α- and β-actin in subcutaneous tissue fibroblasts ex vivo. Normal fibroblasts uniformly exhibited α-smooth muscle actin (α-SMA) immunoreactivity. Unlike cultured fibroblasts and smooth muscle cells, α-SMA in these fibroblasts was not in F-actin form (indicated by lack of phalloidin co-localization) nor was it organized into distinct stress fibers. The lack of stress fibers and fibronexus was confirmed by electron microscopy, indicating that these cells were not myofibroblasts. In unstretched tissue, the pattern of α-actin was diffuse and granular. With tissue stretch (30 min), α-actin formed a star-shaped pattern centered on the nucleus, while β-actin extended throughout the cytoplasm including lamellipodia and cell cortex. This dual response pattern of α- and β-actin may be an important component of cellular mechanotransduction mechanisms relevant to physiologic and therapeutic mechanical forces applied to connective tissue.

Keywords Subcutaneous tissue · Actin · Mechanical stress · Mechanotransduction · Fibroblast

H. M. Langevin (✉) · K. N. Storch · M. J. Cipolla
Department of Neurology, Given C423,
University of Vermont College of Medicine,
89 Beaumont Ave., Burlington, VT 05405, USA
E-mail: helene.langevin@uvm.edu
Tel.: +1-802-6561001
Fax: +1-802-6568704

S. L. White · T. R. Buttolph
Department of Anatomy and Neurobiology,
University of Vermont College of Medicine,
89 Beaumont Ave., Burlington, VT 05405, USA

D. J. Taatjes
Department of Pathology, Microscopy Imaging Center,
University of Vermont College of Medicine,
89 Beaumont Ave., Burlington, VT 05405, USA

Introduction

"Loose" connective tissue traditionally has been regarded as a passive tissue whose main function is to "bind" body components with one another. Within connective tissue, under normal conditions, fibroblasts are generally considered "static" cells chiefly responsible for manufacturing the extracellular matrix. Although fibroblasts have the ability to transform into mechanically active myofibroblasts in response to injury or chronic mechanical stress, this transformation is thought to require de novo synthesis of alpha smooth muscle actin (α-SMA) (Darby et al. 1990; Desmouliere et al. 1993; Gabbiani 2003; Hinz et al. 2001; Majno et al. 1971). Myofibroblasts are defined by their morphological features differentiating them from fibroblasts: abundant α-SMA-containing microfilament bundles reminiscent of smooth muscle cells SMCs, and specialized extracellular matrix attachments termed microtendons or fibronexus junctions (Ryan et al. 1974; Singer 1979). However, some controversy has surrounded this definition of myofibroblasts, and myofibroblast-like cells have been found in a number of normal tissues (Ehrlich et al. 1999; Eyden 2001; Spector 2001; Tomasek et al. 2002). It is nevertheless generally accepted that, in normal skin and subcutaneous tissue (1) myofibroblasts are absent and (2) fibroblasts do not contain α-SMA.

Fibroblasts in normal connective tissues are considered to be "stress-shielded" by the extracellular matrix, and, therefore, not normally exposed to significant mechanical forces (Tomasek et al. 2002). Our recent findings, however, suggest that fibroblasts in "loose" connective tissue may be exposed to considerably more mechanical forces (less stress-shielded) than previously

recognized. First, we showed that the viscoelastic response of rat subcutaneous tissue to incremental elongation was linear up to 60% strain, and that this tissue had a very low tensile modulus that was close to that of cells (Iatridis et al. 2003). Second, we showed that fibroblasts in subcutaneous tissue formed an extensive interconnected cellular network and responded to short-term tissue stretch (10–120 min) with dynamic, pronounced and reversible changes in cell shape (Langevin et al. 2004, 2005). Fibroblasts in stretched tissue developed a "sheet-like" morphology with extensive cell spreading and lamellipodia. Acupuncture needle manipulation, which also causes tissue stretch via winding and pulling of collagen, causes similar changes in fibroblast morphology involving Rac and Rho signaling as well as actomyosin contractility (Langevin et al. 2006). Fibroblasts, therefore, respond rapidly to changes in their mechanical environment with an active reorganization of the actin cytoskeleton. These results raise intriguing questions regarding the possible role of different actin isoforms in this dynamic cytoskeletal response. In several cultured cell models, Class I (β, γ) and Class II (α) actins have been shown to play distinct roles in cell spreading and contraction, respectively (Herman 1993). Beta-actins concentrate in motile, non-contractile areas of the cell (lamellipodia, membrane ruffles, advancing pseudopods) while alpha-actins are found predominantly in stress fibers or sarcomeric-like structures. Since the response of fibroblasts to tissue stretch involves both spreading and contraction, this suggests that both α- and β-actin may play important roles in this dynamic cytoskeletal response. In this study, whole tissue preparation methods without tissue sectioning, freezing or embedding combined with confocal microscopy have (1) allowed visualization of α-SMA in normal subcutaneous tissue fibroblasts, and (2) revealed a dual pattern of α- and β-actin redistribution in response to tissue stretch.

Materials and methods

Subcutaneous tissue sample preparation

Subcutaneous connective tissue was harvested immediately after death from the abdomen of either C57Black6 male mice (19–21 g) or male Wistar rats (450 g). An 8 cm×3 cm flap containing dermis, subcutaneous muscle and subcutaneous tissue was dissected away from the abdominal wall musculature and excised. Unless otherwise specified, all tissue samples were fixed immediately in either 3% paraformaldehyde (PFA) in phosphate-buffered saline (PBS) for light microscopy; 2.5% glutaraldehyde/1.0% PFA in Millonig's phosphate buffer for electron microscopy; or 0.5% PFA/0.1% glutaraldehyde for immunoelectron microscopy. After fixation, subcutaneous tissue samples (20–30 mm in width, 60–80 mm in length and 20?–?? μm in thickness) were dissected from the dermis and subcutaneous muscle while applying minimal traction on the tissue as previously described (Langevin et al. 2004).

For tissue stretched ex vivo, tissue flaps were excised as above and placed between stainless steel grips as previously described (Langevin et al. 2005) in HEPES-physiological saline solution (HEPES-PSS), pH 7.4 at 37°, containing (mM): NaCl 141.8, KCl 4.7, $MgSO_4$ 1.7, EDTA 0.39, $CaCl_2$ 2.8, HEPES 10.0, KH_2PO_4 1.2, Glucose 5.0. The tissue was elongated at a rate of 1 mm/s by advancing a micrometer connected to the distal tissue grip until a load of 0.02 N was registered and then maintained at that length for 30 min, then immersion-fixed in 3% PFA. Controls without load were placed in grips as described above and incubated for 30 min without tissue elongation.

Cell culture

Primary cultures of explanted mouse aortic vascular SMCs (Absher et al. 1997) were grown in T-75 flasks in Dulbecco's Modified Eagle Medium (Gibco, Carlsbad, CA) with insulin-transferrin-selenium (Gibco, Carlsbad, CA), fetal bovine serum (Hyclone, Logan, UT), and epidermal growth factor (Sigma, St. Louis, MO) at room temperature, unless otherwise indicated. Media was aspirated, 4 ml of versene (Gibco, Carlsbad, CA) was added, and the cells were incubated for 5 min. Versene was then aspirated, and SMCs were treated with 2 ml of trypsin (Gibco, Carlsbad, CA) and incubated for 5 min; 8 ml of growth media was added to the solution to neutralize the trypsin; the cells were counted, diluted to 75,000 cells per ml, and seeded at 1 ml on glass coverslips (Krackler Scientific Inc, Albany, NY). SMCs grown overnight at 37°C with 10% CO_2 were then rinsed in PBS. Cultured cells were fixed in 3% PFA in PBS and processed for microscopy 5–7 days post-plating.

Immunohistochemistry

Immunohistochemistry of tissue or SMCs was performed for detection of α-SMA using indirect immunofluorescence and immunoperoxidase techniques. Primary and secondary antibodies were used in various combinations, as summarized in Table 1. For indirect immunofluorescence, three different primary antibodies to α-SMA were used: mouse monoclonal anti α-SMA antibodies from Sigma (St. Louis, MO) at dilutions of 1:100 or 1:1,000 and Chemicon International (Temecula, CA) at a dilution of 1:10, and mouse monoclonal anti α-SMA-1 (Skalli et al. 1986) at dilutions of 1:50–1:200; in addition, a mouse monoclonal against β-tubulin from Sigma (St. Louis, MO) at a working dilution of 1:50 and a mouse monoclonal against β-actin from Sigma (St. Louis, MO) at a working dilution of 1:200 were used. We used five different secondary antibodies: goat anti-mouse Alexa 488, goat anti-mouse Alexa 568, goat anti-mouse Alexa 647 (Invitrogen, Carlsbad, CA) all at a

Table 1 Source and dilution of antibodies

	Primary antibodies	Source	Dilution
Immunofluorescence	Mouse monoclonal anti α-SMA	Sigma-Aldrich, St Louis, MO	1:100–1:1,000
	Mouse monoclonal anti α-SMA	Chemicon Int., Temecula, CA	1:10
	Mouse monoclonal anti α-SMA-1	University of Geneva, Switzerland	1:50–1:200
	Mouse monoclonal anti β-tubulin	Sigma-Aldrich, St Louis, MO	1:50–1:200
	Mouse monoclonal anti β-actin	Sigma-Aldrich, St Louis, MO	1:200
	Biotinylated mouse monoclonal anti α-SMA-1	University of Geneva, Switzerland	1:50
Immunoperoxidase	Mouse monoclonal anti α-SMA	Sigma-Aldrich, St Louis, MO	1:100
	Mouse monoclonal anti α-SMA-1	University of Geneva, Switzerland	1:10–1:200
	Biotinylated mouse monoclonal anti α-SMA-1	University of Geneva, Switzerland	1:50–1:500
Immunoblot	Mouse monoclonal anti α-SMA	Sigma-Aldrich, St Louis, MO	1:4,000
	Mouse monoclonal anti α-SMA-1	University of Geneva, Switzerland	1:4,000

dilution of 1:200, donkey anti-mouse Cy-5 (Jackson ImmunoResearch Laboratories, West Grove, PA) at a dilution of 1:50 and goat anti-mouse FITC (Southern Biotech, Birmingham, AL) at 1:50 dilution. Immunofluorescence was also performed using a biotinylated mouse monoclonal anti α-SMA-1 (Skalli et al. 1986) at a dilution of 1:50, followed by FITC-streptavidin (Vector Laboratories, Burlingame, CA, USA). For immunoperoxidase techniques, we used a mouse monoclonal anti α-SMA antibody (Sigma, St. Louis, MO, USA) at a dilution of 1:100, as well as a biotinylated (1:50 or 1:500) and non-biotinylated (1:10 or 1:200) mouse monoclonal anti α-SMA-1 antibodies (Skalli et al. 1986).

Indirect immunofluorescence method

After fixation of whole tissue flaps, 1 cm×1 cm subcutaneous tissue samples were dissected from the dermis and mounted on Fisherbrand Superfrost/Plus (Fisher Scientific, Pittsburgh, PA, USA) glass microscope slides. Once on slides, samples were rinsed in PBS/1.0% bovine serum albumim (BSA)/0.1% Triton X-100 for 15 min, followed by two 10 min rinses in PBS/1.0% BSA. For mouse tissue, in order to reduce background staining resulting from using mouse primary antibodies, samples were incubated in Mouse-On-Mouse (M.O.M) blocking reagents (Vector Laboratories, Burlingame, CA, USA) prior to primary antibody incubation according to the manufacturer's instructions. Samples were incubated overnight at 4°C with one of the primary anti α-SMA antibodies, rinsed twice in PBS/1% BSA then incubated with one of the secondary antibodies for 1 h at room temperature. Samples were then further incubated with (1) Texas Red conjugated Phalloidin (4 U/ml; Invitrogen, Carlsbad, CA, USA) at a 1:25 dilution for 40 min at 4°C, and (2) either SYTOXGreen (Invitrogen, Carlsbad, CA) nucleic acid stain (1:5,000 dilution) for 2 min, or 4′,6-diamidino-2-phenylindole, dihydrochloride (DAPI) (Invitrogen, Carlsbad, CA) nucleic acid stain at a dilution of 1:1,000 for 5 min, both at room temperature (RT). Slides were then overlaid with a coverslip using 50% glycerol in PBS with 1% *N*-propylgallate as a mounting medium. Tissue samples were imaged with a Bio-Rad MRC 1024 confocal microscope (Bio-Rad Microsciences, Hercules, CA, USA) using a 60× oil immersion lens (N.A. 1.4) and 488, 568, and 647 nm laser excitations.

Avidin/Biotin immunofluorescence method

Samples were dissected and mounted on slides as above, blocked for endogenous biotin according to the manufacturer's directions (Vector Laboratories, Burlingame, CA, USA) and incubated with a biotinylated anti-α-SMA antibody for 30 min at RT. Samples were then rinsed twice for 5 min in PBS/1.0%BSA and incubated with FITC/streptavidin (Vector Laboratories, Burlingame, CA, USA) for 5 min at RT.

Immunoperoxidase method

Samples were dissected and mounted on slides as above, blocked for endogenous peroxidase activity with 0.3% normal horse serum and 0.3% hydrogen peroxide in PBS for 5 min at RT, rinsed twice for 2 min in PBS, and incubated in avidin/biotin blocking reagents (Vector Laboratories, Burlingame, CA, USA) prior to primary antibody incubation according to the manufacturer's instructions. Samples were rinsed twice for 2 min in PBS, incubated with a biotinylated anti-α-SMA antibody for 30 min at RT, rinsed twice again for 2 min in PBS, and incubated with Vectastain followed by peroxidase substrate solution according to the manufacturer's directions (Vector Laboratories, Burlingame, CA, USA).

Antibody blocking experiments

Subcutaneous tissue samples or SMCs were stained using the indirect immunofluorescence technique as above: incubated with anti α-SMA antibodies (Sigma, 1:100–1:1,000) or α-SMA-1 (Skalli et al. 1986) (1:10–1:200). To block the antibody, the N-terminal α-SMA decapeptide (gift from Dr Christine Chaponnier, Universtity of Geneva, Switzerland) was pre-incubated with the α-SMA antibody in M.O.M. Diluent at a final concentration of 100 μg/ml for 1 h prior to staining. Con-

trol samples were incubated with the primary antibody without peptide pre-incubation.

Electron microscopy

Subcutaneous tissue samples were fixed for 1 h at 4°C in a mixture of 2.5% glutaraldehyde, 1.0% PFA in Millonig's phosphate buffer. Following three rinses in buffer, the tissue pieces were encapsulated in 2% agarose (Sea Prep ultra low gelling temperature; Biowhitaker Molecular Applications, Rockland, ME, USA) to maintain stability and orientation. The agarose was solidified by soaking for 15 min in the same fixative as above. Cultured SMCs were fixed in a mixture of 2.5% glutaraldehyde and 1% PFA in Millonig's buffer for 45 min at 4°C. Following fixation, both tissue pieces (in agarose) and cells were postfixed in 1% OsO_4, dehydrated through a graded series of alcohols, and embedded in Spurr's hydrophobic plastic resin. Ultrathin sections were cut with a diamond knife, retrieved onto copper grids, post-stained with uranyl acetate and lead citrate, and finally examined in a JEOL 1210 transmission electron microscope operating at 60 kV.

Immunoelectron microscopy

Subcutaneous tissue pieces were mildly fixed in a 2.5% PFA/0.1% glutaraldehyde combination, followed by low temperature dehydration and embedding in the hydrophilic resin Lowicryl K4M (Abdullah et al. 1991). Antigenic sites for α-SMA were localized with the protein A-gold technique as previously described (Roth and Taatjes 1998).

Immunoblotting experiments

Mouse subcutaneous tissue was dissected and excised as described above. All adipose tissue and blood vessels visible under a dissecting microscope were excised from the tissue. Since subcutaneous tissue itself does not have a capillary bed, this method minimizes contamination of the tissue with vascular SMCs. This method also prevents sample contamination with enteric SMCs, since the abdominal wall remains intact throughout the dissection of the sample. Mouse subcutaneous and aorta tissues (used as controls) were homogenized in Chaps Cell Extract Buffer (Cell Signaling Technology, Beverly, MA, USA) plus a protease inhibitor cocktail (Sigma, St. Louis, MO, USA) using pestles and tubes (Bel-Art Products, Pequannock, NJ, USA) in conjunction with MicroRNA beads (Mo Bio Laboratories, West Carlsbad, CA). Total protein concentration was determined using Coomassie Plus Protein Assay Reagent (Pierce Biotechnology, Rockford, IL). Protein extracts were diluted 1:2 with SDS sample buffer (Invitrogen, Carlsbad, CA) containing 5% 2-mercaptoethanol. The extracts were heated to 95°C for 10 min. After centrifugation, the samples were loaded onto a 16% precast tris-glycine gel (Invitrogen, Carlsbad, CA, USA) and electrophoresed at 125 V, 35 mA, and 5 W for 2 h. Proteins were transferred to Immun-Blot PVDF membrane (Life Science Research, Hercules, CA, USA) at 25 V, 135 mA, and 17 W for 2 h. The membrane was sectioned four ways, then was blocked for 1 h in 1:2 PBS/AquaBlock (East Coast Biologics, North Berwick, ME, USA). The four sections of the blot were incubated overnight at 4°C with mouse anti α-SMA at a dilution of 1:4,000 (Sigma, St. Louis, MO, USA or Universtity of Geneva, Switzerland) with two of the blot sections being co-incubated with the N-terminal α-SMA decapeptide at a dilution of 1:1,000 (Universtity of Geneva, Switzerland). The blots were incubated with a goat anti-mouse Alexa Fluor 700 secondary antibody (Invitrogen, Carlsbad, CA, USA). Bands were detected using an Odyssey infrared scanner (LI-COR Biotechnology, Lincoln, NE).

Results

Tissue fixed immediately after excision

Light microscopy and immunoblots

Mouse subcutaneous tissue fibroblasts stained positively for α-SMA with both immunofluorescence and immunoperoxidase methods (Fig. 1a–d). Similar results were obtained with immunofluorescence using three different primary and five different secondary antibodies, as well as with immunofluorescence using a biotinylated primary antibody followed by streptavidin (Table 1). All results shown were obtained with the primary α-SMA antibody from Sigma. A similar pattern of α-SMA staining was seen in rat subcutaneous tissue as well as in mouse dermis (results not shown). In mouse tissue, α-SMA immunoreactivity was blocked by pre-incubation of the antibody with the N-terminal α-SMA decapeptide (Fig. 2). Immunoblots of mouse subcutaneous tissue and aorta both showed a single immunoreactive band at the expected location corresponding to α-SMA and blocked by the α-SMA peptide (Fig. 3).

In tissue fixed immediately after excision, α-SMA immunoreactivity extended throughout most of the cytoplasm, including some staining along cell processes (Fig. 1a, c). The pattern of α-SMA staining appeared mostly diffuse and granular rather than filamentous. Staining for α-SMA did not co-localize with phalloidin which stained predominantly cortical actin. Neither α-SMA nor phalloidin staining suggested the presence of cytoplasmic stress fibers as typically seen in myofibroblasts and cultured fibroblasts.

In contrast, staining of cultured mouse aortic vascular SMCs using the same method showed clearly demarcated α-SMA-positive stress fibers (Fig. 4a) with

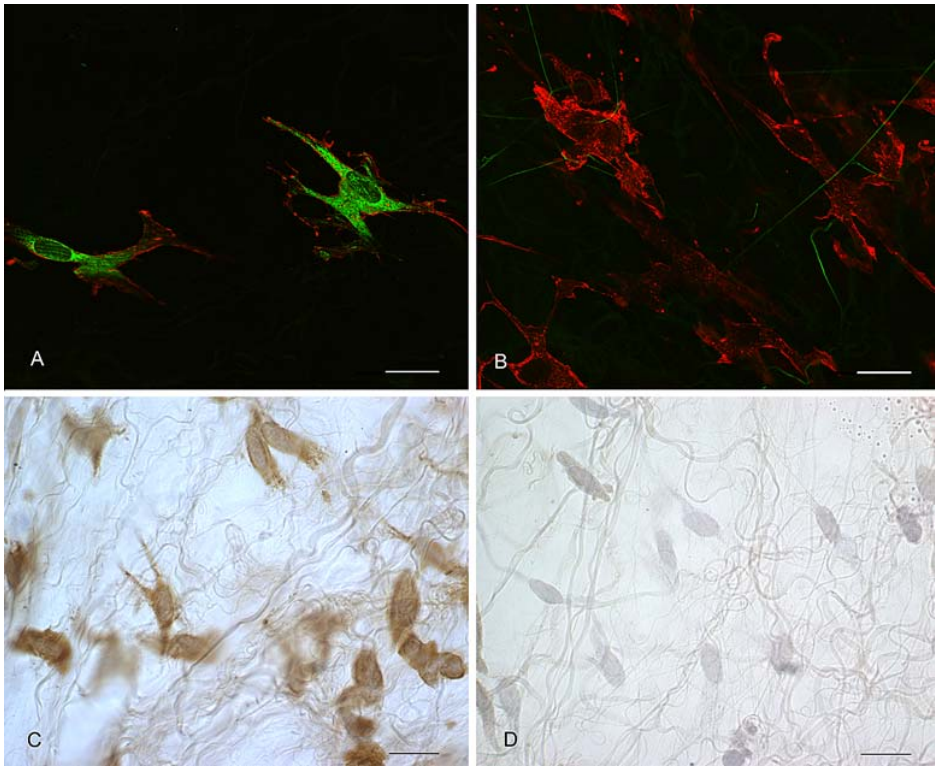

Fig. 1 Immunohistochemical staining of mouse subcutaneous whole tissue mounts. **a**, **b** Immunofluorescence staining with anti α-SMA primary antibody (*green*), counterstained with phalloidin (*red*) imaged with confocal microscopy (**a**), compared with no-primary control (**b**). **c**, **d** Immunoperoxidase staining for α-SMA of mouse subcutaneous tissue counterstained with hematoxylin imaged with light microscopy (**c**) compared with no-primary control (**d**). *Scale bars* 20 μm

extensive co-localization of the α-SMA with phalloidin (Fig. 4b). This α-SMA staining was completely abrogated by pre-absorption of the antibody with the α-SMA peptide (Fig. 4c, d).

Electron microscopy

Conventional transmission electron microscopy and immunoelectron microscopy corroborated the absence of intracytoplasmic stress fibers or fibronexus complexes in mouse subcutaneous tissue fibroblasts. Figure 5 shows a subcutaneous tissue fibroblast imaged with electron microscopy in which no stress fibers or cytoplasmic filaments were detected (see inset to Fig. 5). No α-SMA antigenic sites were detected by the protein A-gold technique (not shown). Intense colloidal gold particle staining for α-SMA was observed over vascular smooth muscle tissue cells fixed and processed in an identical manner as the subcutaneous tissue (not shown), demonstrating the reliability of the technique.

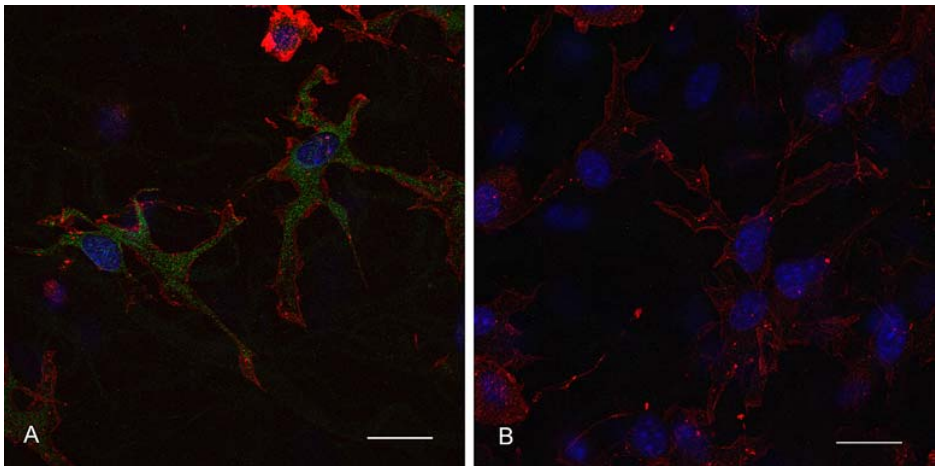

Fig. 2 Antibody blocking experiment. Immunohistochemical staining of mouse subcutaneous tissue for α-SMA blocked with N-terminal α-SMA decapeptide (**b**) compared with a non-blocked control (**a**). Cells are counterstained with phalloidin (*red*) and DAPI (*blue*). All fields were imaged with confocal microscopy. *Scale bars* 20 μm

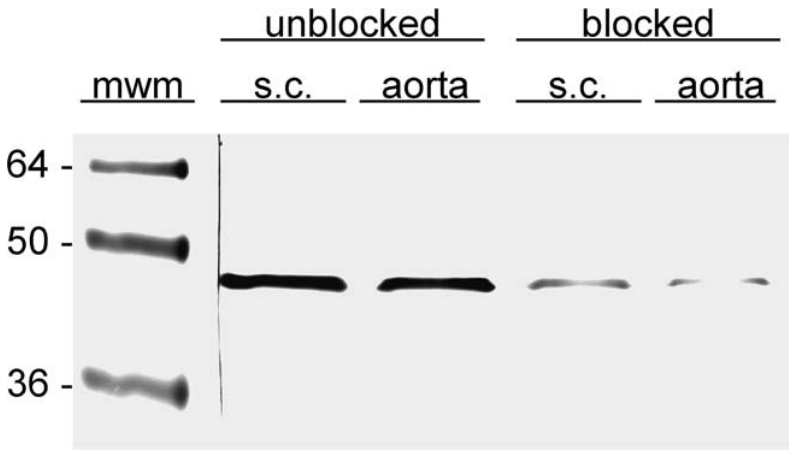

Fig. 3 Immunoblot of mouse subcutaneous tissue (s.c.) and aorta for α-SMA with and without pre-incubation of the α-SMA primary antibody with the N-terminal α-SMA decapeptide. For both blocked and unblocked conditions, the amount of protein loaded was 20 μg and 5 μg for subcutaneous tissue and aorta samples, respectively

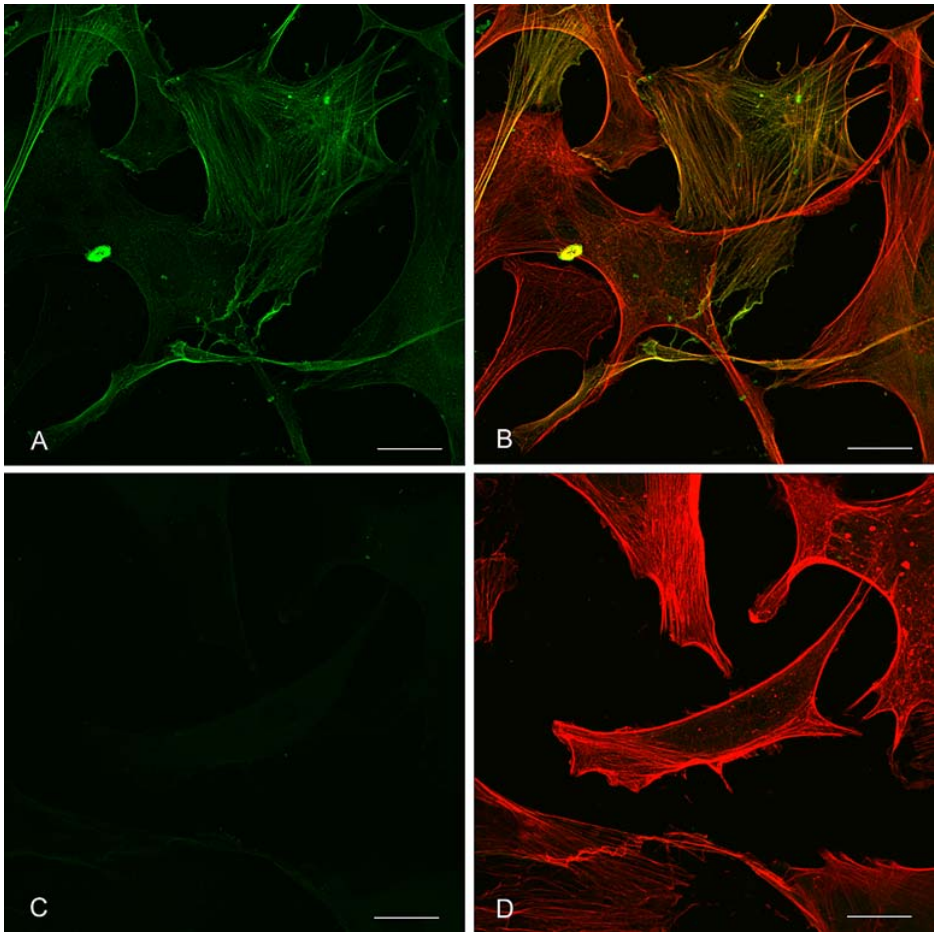

Fig. 4 **a**, **b** Immunohistochemical staining of cultured vascular smooth muscle cells for α-SMA (*green*) (**a**) and α-SMA with phalloidin (*red*) (**b**). **c**, **d** Staining with α-SMA antibody blocked with N-terminal α-SMA decapeptide without phalloidin (**c**) and with phalloidin (**d**). All fields were imaged with confocal microscopy. *Scale bars* 20 μm

Tissue stretched ex vivo

In response to tissue stretched ex vivo for 30 min, fibroblasts became larger, flatter and ''sheet-like'' (Fig. 6) consistent with our previous report (Langevin et al. 2005). In stretched tissue, the fibroblasts' thin cytoplasmic lamellipodia were faintly visible with conventional hematoxylin/eosin staining and light microscopy (Fig. 6b), but became readily apparent with immunohistochemistry and confocal microscopy (Fig. 6d, f, h). Alpha-actin in stretched tissue assumed a ''star-shaped'' pattern centered on the nucleus (Fig. 6d) with little

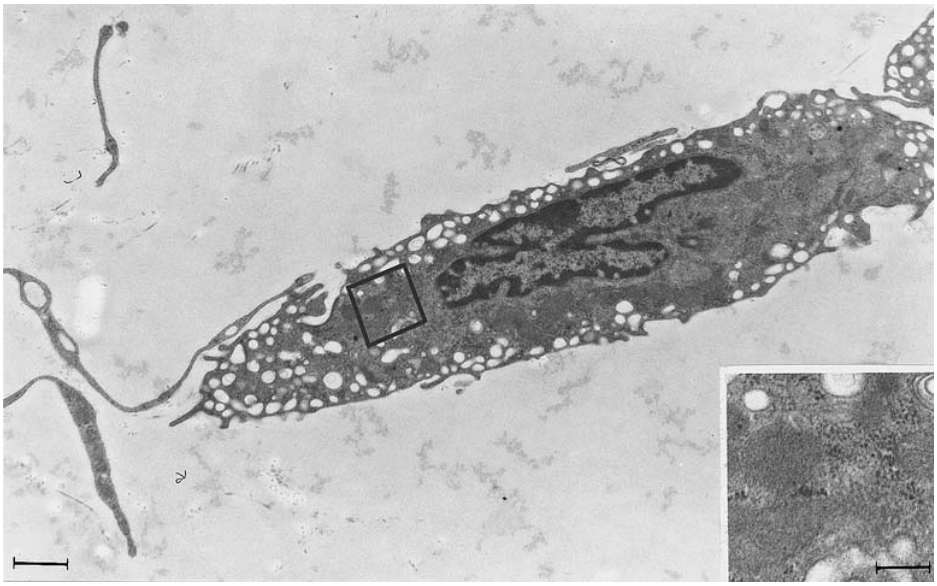

Fig. 5 Electron microscopic imaging of mouse subcutaneous tissue fibroblast showing lack of stress fibers and fibronexus junctions. *Scale bars* Low mag scale bar 0.9524 μm; High mag insert scale bar 0.25 μm

staining of the cell periphery. This was in contrast to the diffuse cytoplasmic α-SMA staining seen with no stretch (Fig. 6c). In both stretched and unstretched tissue, there was little co-localization of α-actin with phalloidin (Fig. 6c, d). However, the pattern of α-actin both with and without stretch was remarkably similar to that of β-tubulin (Fig. 6c–f). Beta-actin, on the other hand, extended throughout the cell cytoplasm including the cell cortex (more visible in stretched tissue) and showed no perinuclear accumulation with stretch (Fig. 6g, h). As expected, there was extensive co-localization between β-actin and phalloidin (not shown).

Discussion

Our results show that normal mouse subcutaneous tissue fibroblasts contain both α- and β-actin, and that both actin isoforms are involved differentially in the dynamic response of fibroblasts to tissue stretch. Alpha-actin appeared to move centripetally in response to stretch, organizing around the nucleus in a star-shaped pattern (Fig. 6c, d). This stretch-induced α-actin pattern suggests the formation of stress fiber-like structures but without classical actin polymerization (indicated by the absence of phalloidin co-localization). The close resemblance between the change in α-actin and β-tubulin patterns with and without stretch further suggests participation of α-actin in active cytoskeletal reorganization. In contrast to α-actin, β-actin extended out into newly formed lamellipodia and cortical actin in response to the same mechanical stimulus. These dual, seemingly opposed actions of Class I and Class II actin types (α-actin contracting inward and β-actin extending outward) are reminiscent of the well-described "tug of war" phenomenon involving front versus rear portions of migrating cells (Small 1988). In contrast to migrating cells, however, fibroblasts in stretched connective tissue appear to expand and internally contract in multiple directions, as if involved in a multidirectional tug of war causing accumulation of internal tension rather than cell movement. The action of α- and β-actin thus may be part of a complex mechanism allowing fibroblasts to actively participate in the regulation of connective tissue tension (Brown et al. 1996).

We used several staining techniques to show the presence of α-SMA in subcutaneous connective tissue fibroblasts in both mice and rats. Both immunofluorescence with several different primary and secondary antibodies, as well as immunoperoxidase showed positive α-SMA staining (Fig. 1). In addition, the blocking antibody to α-SMA completely prevented α-SMA staining, the specificity of which was confirmed by Western blot. Despite the presence of α-SMA, we saw no evidence indicating that the fibroblasts were myofibroblasts as indicated by the absence of cytoplasmic stress fibers or fibronexus junctions by electron microscopy. In contrast, cultured SMCs showed distinct α-SMA staining organized into stress fiber bundles that co-localized with phalloidin. Taken together these results strongly suggest that subcutaneous tissue fibroblasts contain α-SMA that is not organized into distinct fibers. The discrepancy between our results and previous reports of negative α-SMA staining in normal dermis and subcutaneous tissue may be explained by differences in methods, as previous reports used frozen tissue sections (Gabbiani et al. 1973, 1978). It is also possible that the concentration of α-SMA is lower in subcutaneous tissue fibroblasts than in myofibroblasts. This is also suggested by our negative findings using immunoelectron microscopy. Thus low concentrations of α-SMA in fibroblasts may have been detectable with immunofluorescence and light microscopy, but not with the immunogold methods which may be less sensitive since no signal amplification

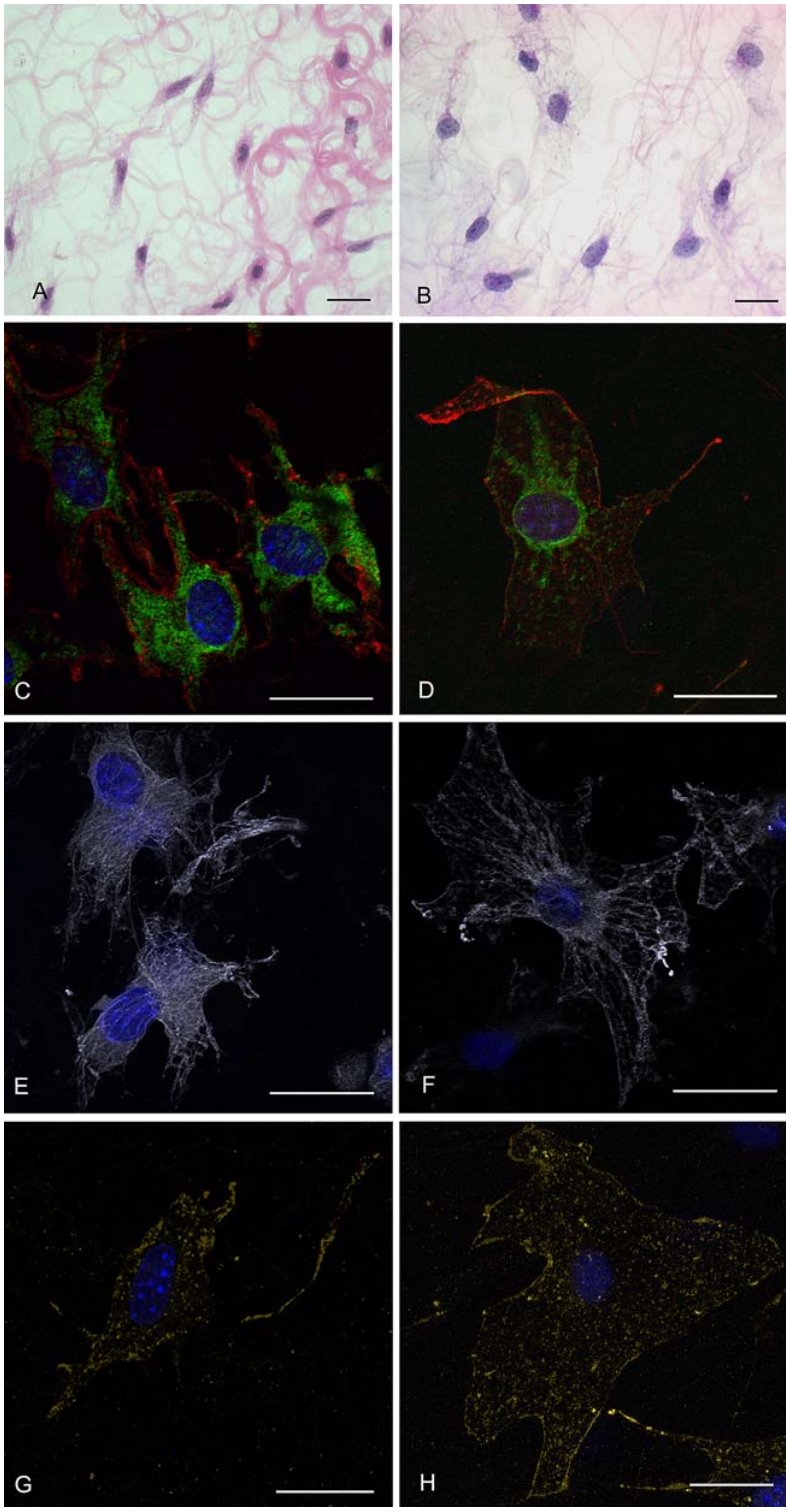

Fig. 6 Effect of tissue stretch on mouse subcutaneous tissue fibroblasts. Mouse subcutaneous tissue was incubated for 30 min without stretch (*left column*: **a**, **c**, **e**, **g**) and with stretch (*right column*: **b**, **d**, **f**, **h**). **a**, **b** Hematoxylin/Eosin stain with light microscopy. **c**, **d** Immunohistochemical staining for α-SMA (*green*) counterstained with phalloidin (*red*). **e**, **f** Immunohistochemical staining for β-tubulin (*white*). **g**–**h** Immunohistochemical staining for β-actin (*yellow*). Fields **c**–**h** were imaged with confocal microscopy and DAPI (*blue*) was used to stain cell nuclei. *Scale bars* 20 μm

occurs as with indirect immunofluorescence methods. Although we cannot completely rule out α-SMA antibody cross-reactivity with another molecule, our results as a whole strongly suggest that α-SMA is indeed present in normal connective tissue fibroblasts.

In summary, the results of this study support our previous findings demonstrating that fibroblasts have a more elaborate repertoire of responses to mechanical stress than was previously realized (Langevin et al. 2005, 2006). Short-term mechanical stress (minutes to hours)

leads to α-and β-actin redistribution and rapid cytoskeletal remodeling that may play an important role in the regulation of connective tissue tension. This is in contrast to the response of fibroblasts to long-term mechanical stress (days to weeks) and/or injury causing increased α-actin synthesis and transformation into a contractile myofibroblast phenotype. Stretch-induced fibroblast cytoskeletal remodeling, as shown in this study, may play an important role in connective tissue responses to normal movement, posture and exercise, as well as mechanical forces applied therapeutically.

Acknowledgements The authors thank Dr. Christine Chaponnier for the generous gift of antibodies and α-SMA peptide, as well as many helpful discussions, Drs. David Schneider and Robert Kelm for the kind gift of SMCs, Nicole Bishop and Heidi Taatjes for technical assistance, as well as Nicole A. Bouffard for help with manuscript preparation. We also thank Drs. Guido Majno, Isabelle Joris and Robert Kelm for their insight and advice. This work was funded in part by the NIH Center for Complementary and Alternative Medicine Research Grant RO1-AT01121 and by NIH Grant P20 RR16435 from the COBRE Program of the National Center for Research Resources. Its content is solely the responsibility of the authors and do not necessarily represent the official views of the National Institutes of Health.

References

Abdullah AM, Nazer H, Atiyeh M, Ali MA (1991) Congenital hepatic fibrosis in Saudi Arabia. J Trop Pediatr 37:240–243

Absher PM, Schneider DJ, Baldor LC, Russell JC, Sobel BE (1997) Increased proliferation of explanted vascular smooth muscle cells: a marker presaging atherogenesis. Atherosclerosis 131:187–194

Brown RA, Talas G, Porter RA, McGrouther DA, Eastwood M (1996) Balanced mechanical forces and microtubule contribution to fibroblast contraction. J Cell Physiol 169:439–447

Darby I, Skalli O, Gabbiani G (1990) Alpha-smooth muscle actin is transiently expressed by myofibroblasts during experimental wound healing. Lab Invest 63:21–29

Desmouliere A, Geinoz A, Gabbiani F, Gabbiani G (1993) Transforming growth factor-beta 1 induces alpha-smooth muscle actin expression in granulation tissue myofibroblasts and in quiescent and growing cultured fibroblasts. J Cell Biol 122:103–111

Ehrlich HP, Keefer KA, Myers RL, Passaniti A (1999) Vanadate and the absence of myofibroblasts in wound contraction. Arch Surg 134:494–501

Eyden B (2001) The myofibroblast: an assessment of controversial issues and a definition useful in diagnosis and research. Ultrastruct Pathol 25:39–50

Gabbiani G (2003) The myofibroblast in wound healing and fibrocontractive diseases. J Pathol 200:500–503

Gabbiani G, Ryan GB, Lamelin JP, Vassalli P, Majno G, Bouvier CA, Cruchaud A, Luscher EF (1973) Human smooth muscle autoantibody. Its identification as antiactin antibody and a study of its binding to "nonmuscular" cells. Am J Pathol 72:473–488

Gabbiani G, Chaponnier C, Huttner I (1978) Cytoplasmic filaments and gap junctions in epithelial cells and myofibroblasts during wound healing. J Cell Biol 76:561–568

Herman IM (1993) Actin isoforms. Curr Opin Cell Biol 5:48–55

Hinz B, Celetta G, Tomasek JJ, Gabbiani G, Chaponnier C (2001) Alpha-smooth muscle actin expression upregulates fibroblast contractile activity. Mol Biol Cell 12:2730–2741

Iatridis JC, Wu J, Yandow JA, Langevin HM (2003) Subcutaneous tissue mechanical behavior is linear and viscoelastic under uniaxial tension. Connect Tissue Res 44:208–217

Langevin HM, Cornbrooks CJ, Taatjes DJ (2004) Fibroblasts form a body-wide cellular network. Histochem Cell Biol 122:7–15

Langevin HM, Bouffard NA, Badger GJ, Iatridis JC, Howe AK (2005) Dynamic fibroblast cytoskeletal response to subcutaneous tissue stretch ex vivo and in vivo. Am J Physiol Cell Physiol 288:C747–756

Langevin HM, Bouffard NA, Badger GJ, Churchill DL, Howe AK (2006) Subcutaneous tissue fibroblast cytoskeletal remodeling induced by acupuncture: evidence for a mechanotransduction-based mechanism. J Cell Physiol (in press)

Majno G, Gabbiani G, Hirschel BJ, Ryan GB, Statkov PR (1971) Contraction of granulation tissue in vitro: similarity to smooth muscle. Science 173:548–550

Roth J, Taatjes DJ (1998) Tubules of the trans Golgi apparatus visualized by immunoelectron microscopy. Histochem Cell Biol 109:545–553

Ryan GB, Cliff WJ, Gabbiani G, Irle C, Montandon D, Statkov PR, Majno G (1974) Myofibroblasts in human granulation tissue. Hum Pathol 5:55–67

Singer II (1979) The fibronexus: a transmembrane association of fibronectin-containing fibers and bundles of 5 nm microfilaments in hamster and human fibroblasts. Cell 16:675–685

Skalli O, Ropraz P, Trzeciak A, Benzonana G, Gillessen D, Gabbiani G (1986) A monoclonal antibody against alpha-smooth muscle actin: a new probe for smooth muscle differentiation. J Cell Biol 103:2787–2796

Small JV (1988) The actin cytoskeleton. Electron Microsc Rev 1:155–174

Spector M (2001) Musculoskeletal connective tissue cells with muscle: expression of muscle actin in and contraction of fibroblasts, chondrocytes, and osteoblasts. Wound Repair Regen 9:11–18

Tomasek JJ, Gabbiani G, Hinz B, Chaponnier C, Brown RA (2002) Myofibroblasts and mechano-regulation of connective tissue remodelling. Nat Rev Mol Cell Biol 3:349–363